Self-Reconfigurable RFID Reader Antenna

Pavel Nikitin
Honeywell
Lynnwood, WA, USA
nikitin@ieee.org

***Abstract*— This paper presents a self-reconfigurable switched beam RFID reader antenna concept and its experimental implementation. The specific antenna presented in this paper is a planar 2-element Yagi array with a parasitic element loaded with a self-oscillating switching circuit powered wirelessly, by the antenna signal itself. Once this reader antenna is fed with RF signal of sufficient power, the circuit starts oscillating, switching between the two complex impedance values, and thus changing the antenna radiation pattern. We describe a theory of operation, including modeling and simulation, and present a prototype of such an antenna operating at 900 MHz with two distinct switched beams and a peak gain of 4.5 dBi.**

I. Introduction

There exists a strong interest in reconfigurable antennas for RFID readers, especially beam steering antennas that can be used, for example, for better tag localization [1-7]. In general, antennas with electronically reconfigurable directive patterns (such as phased arrays) have long been known and used [8-13]. Such antennas typically have elements which are electronically switched using either some RF switches or variable components (such as voltage controlled capacitors) that control the antenna properties [14]. Such antennas require either DC bias lines or DC biased RF feeds to control and power the switches [15]. Typical examples of such antennas are electronically steerable arrays with passive array radiators, also known as ESPAR [16-27].

Recently, a theoretical concept of a wirelessly reconfigurable antenna was proposed [28] where wirelessly powered switches on parasitic elements are controlled by modulating signals embedded into the antenna transmission. The difficulty with practically implementing that concept is the need for additional protocol overhead to control the switches and the complexity of such intelligent switches.

In this paper, another concept is proposed: a self-reconfigurable antenna where a parasitic element is loaded with self-oscillating switching circuit. This RF powered circuit periodically switches between the two complex impedance values, essentially turning the parasitic element into either a director or a reflector (this effect of reactive load on parasitic elements in arrays is well known in antenna literature [12, 19, and 20]). When such antenna is fed with RF signal, it "comes alive" and starts oscillating, switching between the two radiation patterns.

We present a first practical implementation of such antenna: a 2-element planar Yagi array which can be used as RFID reader antenna with two distinct switched beams that, for example, automatically scan for tags in two different directions. The idea presented in this paper has been described in our pending patent application [29] but to the best of our knowledge, this is the first time such antenna concept is described in IEEE literature.

II. Design

A. General considerations

Known planar Yagi implementations of reconfigurable switched beam antennas have three or more antenna elements and require two or more switches to operate [30-34]. In our case, we need to be able to switch antenna beams using only one wirelessly powered and self-oscillating switch. Thus a 2-element Yagi antenna was chosen, consisting of two elements of different length as shown in Figure 1. The circuit that loads the parasitic element oscillates between the two complex impedance values, essentially turning it into either a director or a reflector and steering the direction of the main antenna beam by 180 degrees.

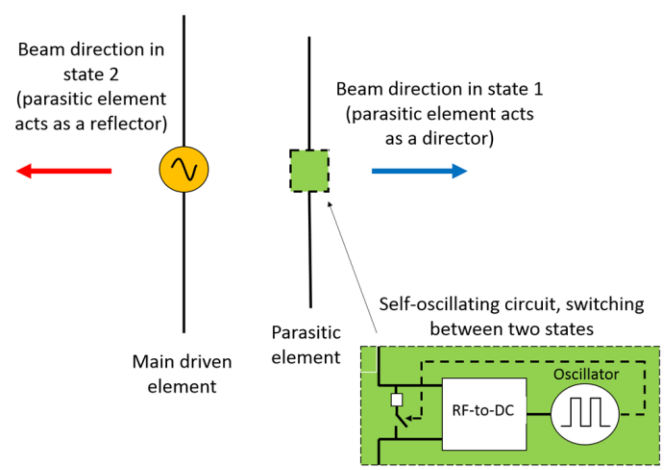

Figure 1. Self-reconfigurable 2-element Yagi antenna with switching circuit on parasitic element.

Similar to RFID tag design process, we will first define and design an RF circuit and then will define and design an antenna to operate with it.

B. Circuit design

The circuit we would like to have must be an RF-powered circuit that self-oscillates to periodically turn on and off the front end modulator. While there certainly exists more than one way to implement such a circuit, one straightforward approach is to create an RF-to-DC power harvesting circuit feeding the resistor-capacitor (RC) timing circuit whose voltage is sensed by a comparator that periodically triggers and discharges the storage capacitor by turning on the PIN diode on the front end. The general circuit block diagram is shown in Figure 2.

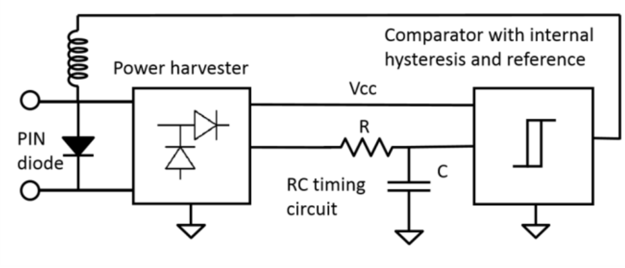

Figure 2. Block diagram of the switching circuit.

The detailed circuit schematic is shown in Figure 3. The power harvesting circuit is a standard multi-stage RF-to-DC converter used in many RFID tag front ends and wireless power harvesting circuits [35, 36]. The output of the first stage charges the timing circuit (defined by resistors R2 and R3 and capacitor C7) while two additonal stages provide higher supply voltage to the comparator U1. The latter is set with hysteresis and reference voltage thresholds defined by resistors R4 and R5 and comparator internal diode. The hysteresis is needed so that that the circuit oscillates instead of settling into a stable state. When the voltage on the capacitor C7 exceeds the set threshold, the comparator trips and turns on the PIN diode D1 (biased via resistor R1 and inductor L1) which greatly reduces the amount of RF power available to RF-to-DC converter and brings down the voltage on C4. As a result, the capacitor C7 starts discharging and once the voltage drops low enough, the comparator trips back and the cycle repeats. Thus the circuit oscillates and modulates its RF input port, similar to an RFID tag IC modulating its antenna port.

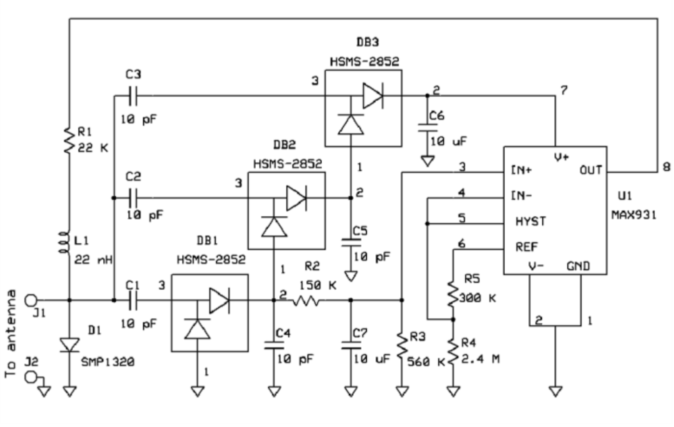

Figure 3. Switching circuit schematic.

While there exist many options for RF switches [37] but PIN diode [38, 39] remains the most common element used in reconfigurable antennas [21, 23, 24, 40], so it was used here. This circuit was intentionally designed with standard off-the-shelf components (SMP1320 PIN diode [41], HSMS 2852 Schottky diode pairs [42], MAX931 comparator IC [43], resistors, capacitors, and inductors) so that it can easily be made and studied.

Since the antenna presented here is intended for use with fixed RFID readers with high power, the circuit was intentionally designed to start oscillating at higher power levels. The specific values of the components (such as resistors R5 and R4 that set the 0.3 V hysteresis band centered around internal 1.182 V comparator reference voltage) were selected so that when the circuit is driven with 10 dBm unlodulated RF signal at 900 MHz, it would oscillate with the frequency of approximately 0.5 Hz, spending about 1 second in each switched state. The minimum threshold input RF power required for the circuit to oscillate is about 7 dBm. Changing the frequency or adding modulation affects this threshold because the input impedance of this circuit (just like an input impedance of an RFID chip) is a function of frequency and average absorbed power.

C. Circuit prototype

The switching circuit was prototyped (hand built) on 15 mm x 20 mm breadboard PCB with edge mount SMA RF jack connector (for ease of testing) and is shown in Figure 4 together with SMA male to SMA male adapter that was used to connect it to the antenna.

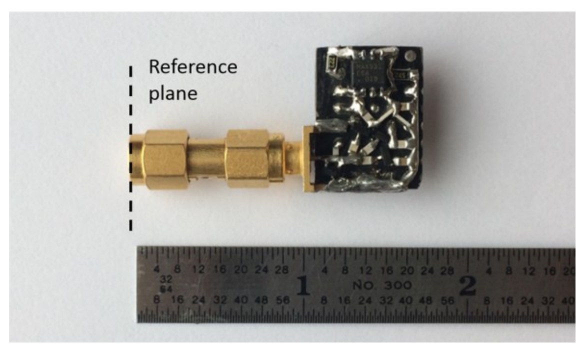

Figure 4. Switching circuit prototype.

Two impedance states of the switching circuit were measured at the reference plane (shown with dashed line in Figure 4) with the network analyzer and are shown on Smith Chart in Figure 5 (state 1 is shown for two network analyzer output power levels, -10 dBm and 10 dBm, while state 2 is shown for one power level, 10 dBm).

Figure 6 shows the impedance matching (power transmission) coefficient calculated using standard equation, often used in RFID [44]:

$$\tau = \frac{4R_g R_l}{\left|Z_g + Z_l\right|^2}\ , \qquad (1)$$

where $Z_g = R_g + jX_g$ is the generator (network analyzer) impedance, and $Z_l = R_l + jX_l$ is the load impedance. As one can see, at 900 MHz the power transmission coefficient is about -3.2 dB, and thus the power absorbed by the circuit in state 1 is about 6.8 dBm.

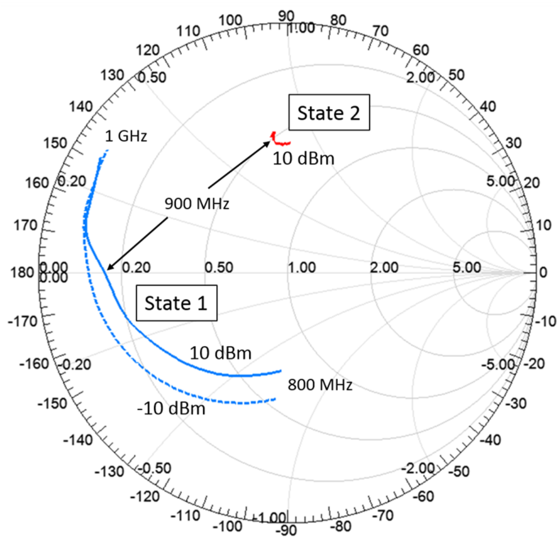

Figure 5. Two impedance states of the switching circuit.

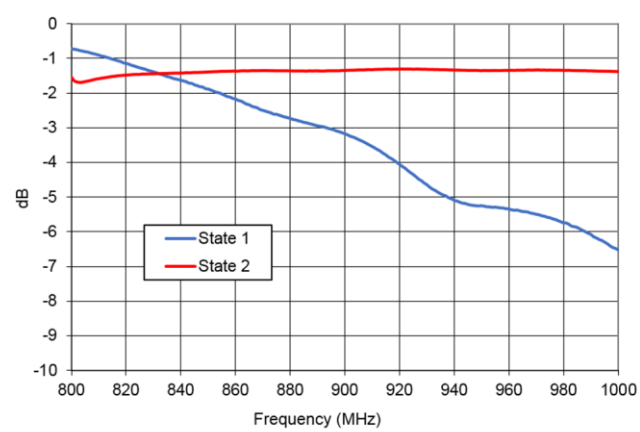

Figure 6. Impedance matching coefficient (network analyzer output power is 10 dBm).

TABLE I. RF SWITCH IMPEDANCE STATES.

State	***State 1***	***State 2***
Complex impedance at 900 MHz	8.15-j1.07 Ohm	27.8+j39.3Ohm
Rseries	8.15 Ohm	27.8 Ohm
Xseries	165 pF	6.95 nH
Rparallel	8.29 Ohm	83.36 Ohm
Xparallel	2.81 pF	10.43 pF
Impedance matching coefficient	-3.17 dB	-1.36 dB

Table I shows the values of the RF switching circuit impedance measured at 900 MHz and 10 dBm power level. The calculation of equivalent parallel circuit values was done using useful online impedance calculator [45]. Those are the values that will be used to design an antenna to operate with.

To confirm that the circuit oscillates properly, we measured the voltage on pin 8 of the comparator U1 while the circuit was driven with 900 MHz 10 dBm unmodulated RF CW signal from the signal generator. This voltage is modulating the PIN diode on the front end. The waveform was recorded with Tektronix TDS 360 oscilloscope (it does not support modern I/O formats, so the photograph of the screen was used to generate the plot in Figure 7).

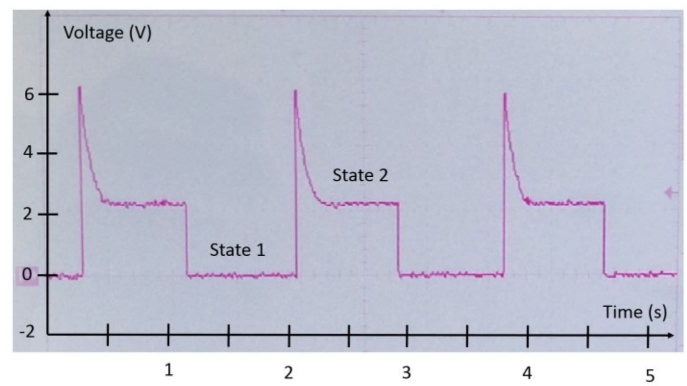

Figure 7. Voltage measured on pin 8 of the comparator U1 when the circuit is driven with 900 MHz 10 dBm signal.

D. *Antenna design*

Now that the input impedance of RF front end of the physical switching circuit (including parasitics) is known from the measurements, a switching antenna can be designed, using two lumped complex load values listed in Table I.

The antenna was designed, modeled and simulated using Ansys HFSS [46]. The antenna model with two edge mount SMA RF connectors is shown in Figure 8. It consists of 140 mm long driven element and 120 mm long parasitic element. Both elements are 5 mm wide planar copper traces, spaced 60 mm apart on 30 mil FR4 substrate (with dielectric permittivity 4.4). Port 1 is the input port of the antenna, and port 2 is where the switching circuit is connected to. The antenna was designed to operate at 900 MHz with connected switching circuit load. Two main considerations in the antenna design were to make sure the antenna can operate with 20 dBm RF source while delivering enough power to the switching circuit and to achieve a significant change in radiation pattern when the circuit is switching between the two states.

Figures 9 and 10 show the radiation patterns in the E- and H-planes for the two different states of the switching circuit listed in Table I. One can see that the peak antenna gain is about 3.5 dBi in state 2 and 4.5 dBi in state 1 (the maximum theoretical gain expected from 2-element Yagi configuration is 5 dBi). Depending on the state of the switch, the antenna pattern switches (rotates) by 180 degrees.

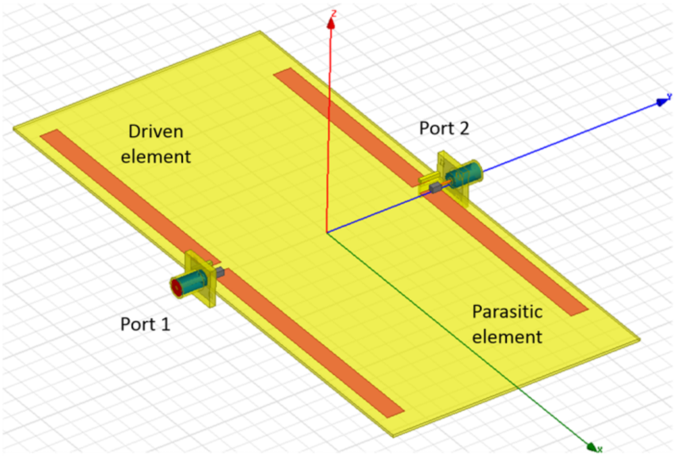

Figure 8. Antenna model in HFSS.

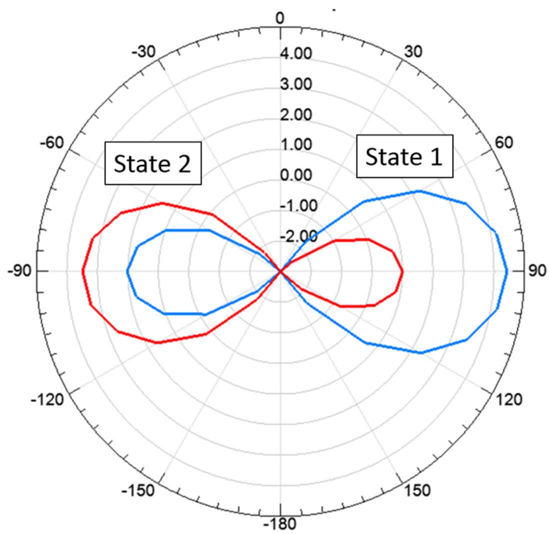

Figure 9. Simulated antenna radiation pattern (realized gain, dBi) at 900 MHz in E-plane (XY-plane) for two states.

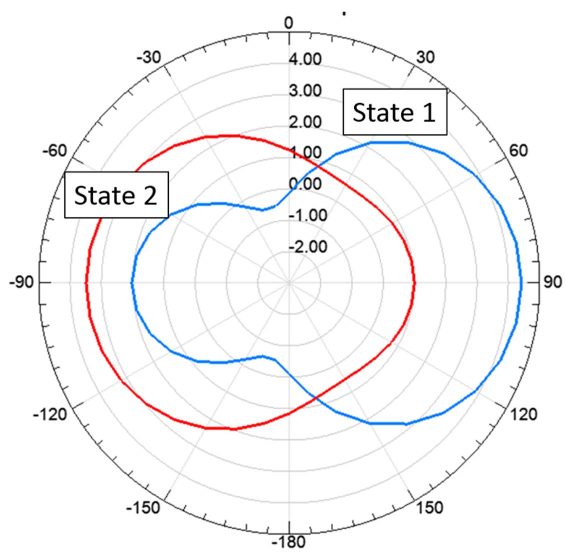

Figure 10. Simulated antenna radiation pattern (realized gain, dBi) at 900 MHz in H-plane (YZ-plane) for two states.

E. Antenna prototype

The antenna was prototyped according to HFSS model, using copper traces on 30 mil FR4 substrate. Prototyped antenna is shown in Figure 11, with the switching circuit connected to port 2.

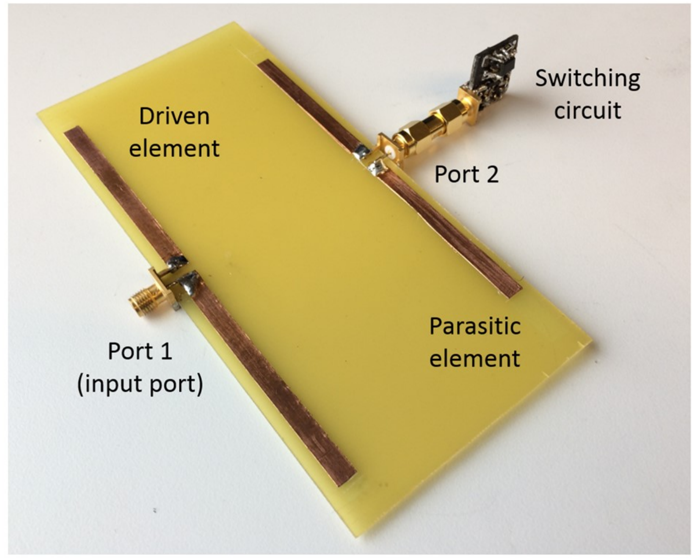

Figure 11. Prototype antenna.

Figure 12 shows both measured and simulated S-parameters of the antenna. As one can see, the results are in good agreement with experimental measurements. To achieve that accuracy, detailed models of SMA RF connectors were used in HFSS.

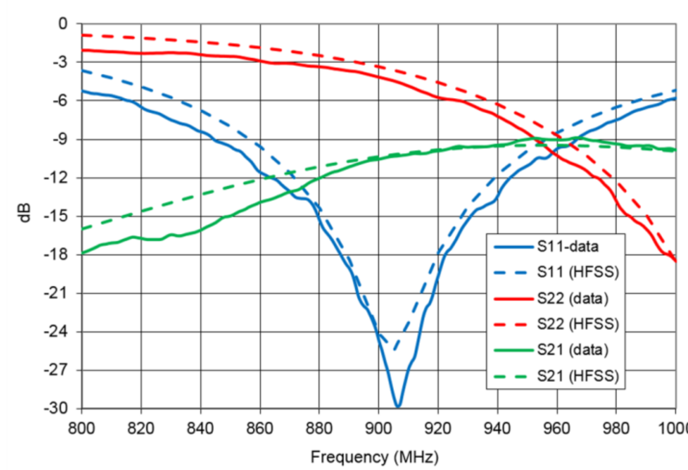

Figure 12. Measured and simulated S-parameters of the antenna.

Figure 13 shows both measured and simulated S11 of the antenna when the antenna is loaded with the switching circuit. Because the maximum output power of the network analyzer is only 10 dBm, in order to perform measurements for state 2 we biased the PIN diode D1 via an external 22 K resistor connected to an external 2 V voltage source. This allowed us to approximate the proper input impedance in state 2, in which the PIN diode is biased (via R1 and L1, see Figure 3) with that voltage (see Figure 7).

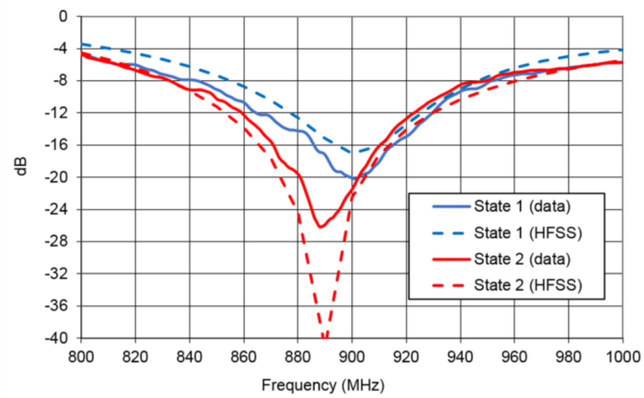

Figure 13. Measured and simulated S11 of the antenna in two states specified in Table I.

Our 2-port antenna loaded with the switching circuit can also be represented as an equivalent circuit shown in Figure 14, for which a transducer power gain G_T can be calculated using well known formula [47, 48]:

$$G_T = \frac{4R_g R_l |Z_{21}|^2}{|(Z_{11} + Z_g)(Z_{22} + Z_l) - Z_{12}Z_{21}|^2} \quad . \tag{2}$$

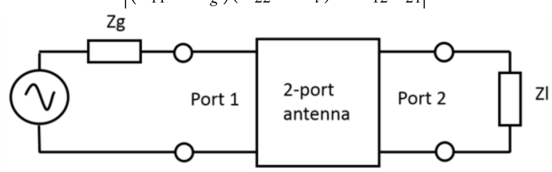

Figure 14. Equivalent circuit of the self-reconfigurable antenna.

Using Z-parameters from simulation, measured load impedance at 10 dBm network analyzer power level (see Figure 5), network analyzer impedance (50 Ohm), and impedance matching coefficient (see Figure 6), we can easily calculate at each frequency the power into the input port of the antenna needed to achieve a specific amount of power absorbed in the switching circuit for each state, as shown in Figure 15. For example, at 900 MHz, where the input RF power is 20 dBm, the power absorbed by the circuit in state 1 is 6.83 dBm.

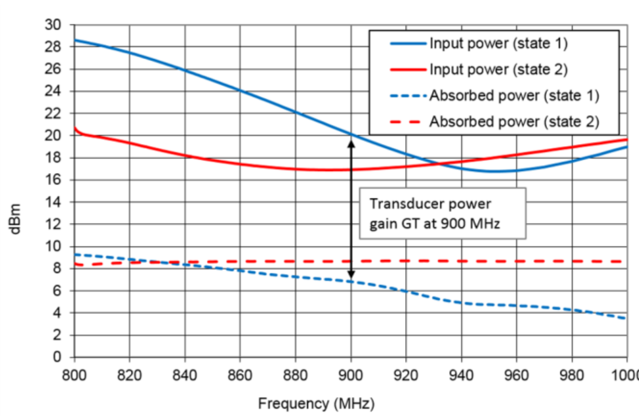

Figure 15. Input power into the antenna needed to achieve specific absorbed power at the switching circuit (in both states). The difference between the two curves for each state is the transducer power gain.

III. VERIFICATION

We first verified the switching beam behavior of our self-reconfigurable antenna prototype by constructing the experimental setup shown in Figure 16. The RF signal generator (HP DSG-E3000A) was transmitting the 20 dBm 900 MHz signal via low-loss coaxial cable into the antenna. The receiving dipole, connected to the RF spectrum analyzer (HP 8593E) was set at a distance of 4 ft (1.2 m) from the center of the antenna. We observed that during the switching cycle the received RF power for maximum gain beam direction (corresponding to state 1) of the self-reconfigurable antenna changed by approximately 3 dB, as expected from the simulated radiation patterns shown in Figures 9 and 10.

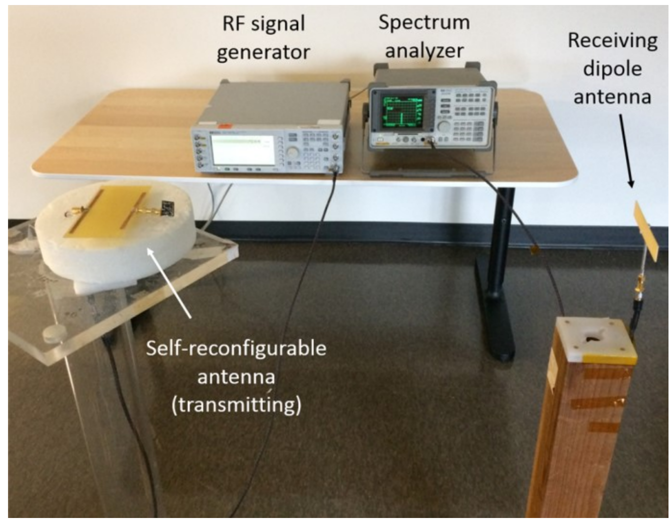

Figure 16. Experimental setup to verify the switching beam behavior of the self-reconfigurable antenna.

We also measured the radiation pattern of the self-reconfigurable antenna using the method described in [49], where a conducted RFID tag is connected to an antenna under test so that the threshold sensitivity and the radiation pattern of the resulting equivalent RFID tag can be measured using standard RFID tag measurement setup.

For that purpose, we used Voyantic Tagformance Pro RFID measurement equipment with automated tag rotation system and linearly polarized patch antenna [50]. The conducted tag was made based on Impinj Monza 2 ASIC, matched to 50 Ohm as shown in Figure 17. The measured return loss and threshold sensitivity of this conducted tag are shown in Figure 18.

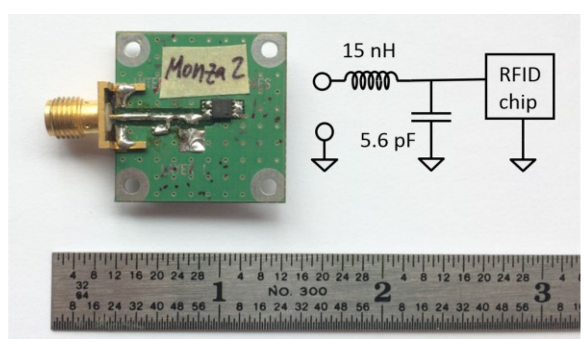

Figure 17. Conducted tag used for pattern measurements.

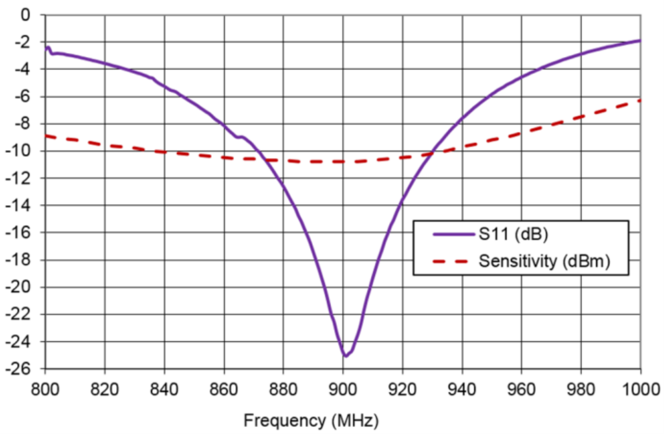

Figure 18. Threshold power sensitivity (dBm) and return loss (dB) of the conducted tag.

For radiation pattern measurements, the conducted tag was connected to port 1 and the switching circuit was connected to port 2 of the self-reconfigurable antenna. In order to properly measure the radiation pattern in state 2, we again needed to approximate the input impedance exhibited by the switching circuit in state 2, where the average voltage on pin 8 of U1 is 2 V (see Figure 7). To do that, we again biased the PIN diode D1 via an external 22 K resistor connected to an external 2 V voltage source – but this time a small 3 V coin cell battery with a resistive divider, placed on the bottom side of our switching circuit board. The diagram and the photograph of the experimental setup are shown in Figure 19.

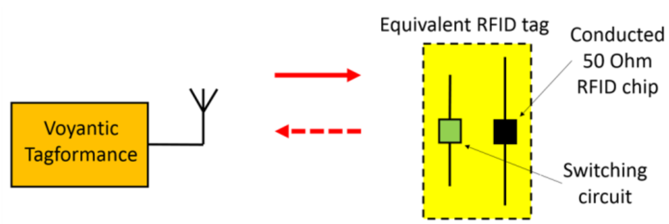

Figure 19. Diagram of the experimental setup to measure the radiation pattern of the self-reconfigurable antenna.

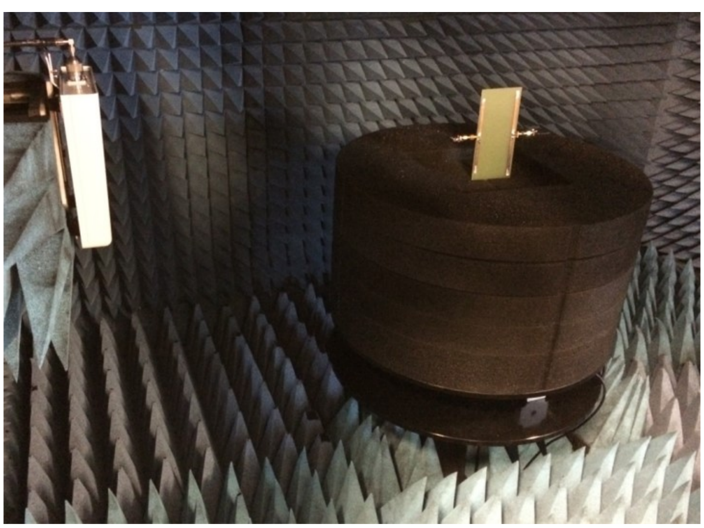

Figure 20. Photograph of the experimental setup to measure the radiation pattern of the self-reconfigurable antenna.

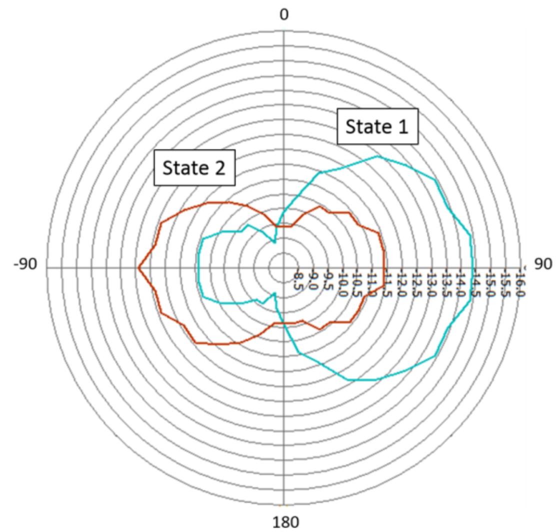

Figure 21. Measured radiation pattern (equivalent RFID tag angular sensitivity, dBm) at 900 MHz in H-plane (YZ-plane).

The radiation pattern of the self-reconfigurable antenna was measured in H-plane using the method described above and is shown in Figure 21. The radial scale is the tag sensitivity, varying from -8 dBm to -16 dBm. As one can see, the measured results are in reasonable agreement with simulations presented in Figure 10. For example, the conducted tag sensitivity at 900 MHz is about -10.5 dBm, and thus measured peak tag sensitivity of -14.5 dBm in state 1 corresponds to antenna gain of about 4 dBi. The switching beam pattern shown in Figure 21 is what this antenna is expected to exhibit when driven with 20 dBm 900 MHz RF signal. These results verify the functionality of the self-reconfigurable antenna prototype presented in this paper.

IV. Discussion and Conclusions

In this paper, we presented a self-reconfigurable antenna concept with a self-oscillating switching circuit powered by the transmitter signal. We implemented it with a 2-element Yagi with a circuit-loaded parasitic element. The antenna automatically switches between the two fixed beam patterns defined by the two impedance states of the circuit, loading the parasitic element. We described a theory of operation and presented experimental results, proving the feasibility and demonstrating the functionality of such antenna.

Since the antenna does not require adding any DC bias control lines or feeds or control signals to operate the switching circuit, it can be used with off-the-shelf readers which makes it especially attractive for use with fixed RFID readers which typically transmit high RF power (up to 30 dBm), more than enough to power the switches on the parasitic elements of such antenna. The proposed concept can also find use in near field reconfigurable RFID antennas for such applications as inventorying goods on shelves and in confined areas [51-55].

Note that the antenna needs a transmitter signal to oscillate and thus is well suited for RFID readers which transmit and receive at the same time, while in the absence of the transmitter signal the antenna radiation pattern in receiving mode will remain fixed.

In the present implementation, the oscillation frequency of the switching circuit depends on the specific values of the circuit components as well as on the input power and the modulation details (modulation depth, average duty cycle, etc.) of the RF signal feeding the antenna. The switching frequency can be made independent of those parameters by using voltage regulators both for the timing circuit and for the comparator. The RF sensitivity of the circuit can be improved by using low power comparator (such as TS881), FET transistor (such as NE25139) as a front end modulator, and better impedance matching. The high frequency transient present during the switching (see Figure 7) can be eliminated with the use of low pass filter and voltage regulators.

The general principle of reactively controlling the parasitic antenna elements [12, 19, 56-58], combined with the concept of RF powered switches on such elements, can be used for other applications beyond RFID, such as reconfigurable Wi-Fi antennas (including MIMO antenna systems [59, 60]) and reflectarrays [61, 62]. Self-reconfigurable antenna concept presented here can also be applied to control other antenna properties besides radiation pattern, such as frequency band [63, 64] or polarization [65, 66]. The same concept can also be applied to other reconfigurable antenna structures, such as patch and microstrip arrays described in [67-69]. Such antennas radiate perpendicular to the plane of the antenna and are very practical since they can be mounted flat on surfaces such as walls.

In general, the RF-powered switching circuit described in this paper can be viewed as a non-linear passive two-terminal electrical component, somewhat similar to memristor whose use for reconfigurable electromagnetic devices has recently been theoretically investigated [70].

The antenna described in this paper can be viewed as a simple but important first step towards building various self-reconfigurable RF devices and systems (antennas, filters, etc.) where available RF power is sufficient to power various circuits that can change their RF properties, thus bringing an additional level of intelligence to RF devices and systems.

References

[1] N. C. Karmakar, S. M. Roy, M. S. Ikram, "Development of Smart Antenna for RFID Reader," IEEE RFID Conference, pp. 65-73, 2008

[2] R. Kronberger, T. Knie, R. Leonardi, U. Dettmar, M. Cremer and S. Azzouzi, "UHF RFID localization system based on a phased array antenna," 2011 IEEE International Symposium on Antennas and Propagation (APSURSI), Spokane, WA, 2011, pp. 525-528

[3] A. Bouzakis and L. Overmeyer, "RFID tag positioning with the aid of an active electronically-steered array," 2012 IEEE 23rd International Symposium on Personal, Indoor and Mobile Radio Communications - (PIMRC), Sydney, NSW, 2012, pp. 2483-2488

[4] H. T. Chou, M. Y. Lee and C. T. Yu, "Implementation scenario of phase array antennas with beam-scan functionality for RFID applications," 2016 10th European Conference on Antennas and Propagation (EuCAP), Davos, 2016, pp. 1-4

[5] D. Wei, W. Hung and K. L. Wu, "A real time RFID locationing system using phased array antennas for warehouse management," 2016 IEEE International Symposium on Antennas and Propagation (APSURSI), Fajardo, 2016, pp. 1153-1154

[6] M. Ould-Elhassen, M. Mabrouk, A. Ghazel and P. Benech, "Improved coverage of phased array antennas used for RFID applications," 2013 IEEE International Symposium on Phased Array Systems and Technology, Waltham, MA, 2013, pp. 553-55

[7] W. S. Lee, S. T. Khang, W. S. Lee, H. S. Tae and J. W. Yu, "Wide-coverage array antenna using a dual-beam switching for UHF RFID applications," 2013 IEEE International Conference on RFID (RFID), Penang, 2013, pp. 36-41

[8] D. Parker and D. C. Zimmermann, "Phased arrays - part 1: theory and architectures," and "Phased arrays-part II: implementations, applications, and future trends," in IEEE Transactions on Microwave Theory and Techniques, vol. 50, no. 3, pp. 678-698, Mar 2002

[9] C. G. Christodoulou, Y. Tawk, S. A. Lane and S. R. Erwin, "Reconfigurable Antennas for Wireless and Space Applications," in Proceedings of the IEEE, vol. 100, no. 7, pp. 2250-2261, July 2012

[10] Chen Sun, A. Hirata, T. Ohira and N. C. Karmakar, "Fast beamforming of electronically steerable parasitic array radiator antennas: theory and experiment," in IEEE Transactions on Antennas and Propagation, vol. 52, no. 7, pp. 1819-1832, July 2004

[11] C. M. Coleman, E. J. Rothwell, J. E. Ross and L. L. Nagy, "Self-structuring antennas," in IEEE Antennas and Propagation Magazine, vol. 44, no. 3, pp. 11-23, Jun 2002

[12] R. Harrington, "Reactively controlled directive arrays," in IEEE Transactions on Antennas and Propagation, vol. 26, no. 3, pp. 390-395, May 1978

[13] D. Peroulis, K. Sarabandi, L. Katehi, "Design of reconfigurable slot antennas," IEEE Trans. on Ant. and Prop., vol. 53, pp. 645-654, 2005

[14] A. E. Fathy et. al., "Silicon-based reconfigurable antennas-concepts, analysis, implementation, and feasibility," IEEE Trans. on Microwave Theory and Techniques, vol. 51, no. 6, pp. 1650-1661, June 2003

[15] J. M. Kovitz, H. Rajagopalan, Y. Rahmat-Samii, "Practical and Cost-Effective Bias Line Implementations for Reconfigurable Antennas," IEEE Antennas and Wireless Prop. Letters, vol. 11, pp. 1552-1555, 2012

[16] G. M. Coutts, R. R. Mansour, S. K. Chaudhuri, "A MEMS-based electronically steerable switched parasitic antenna array," IEEE APS Symposium, vol. 2A, pp. 404-407, Jul. 2005

[17] L. Petit, L. Dussopt, J.-M. Laheurte, "MEMS-Switched Parasitic-Antenna Array for Radiation Pattern Diversity," IEEE Transactions on Antennas and Propagation, vol.54, no.9, pp.2624-2631, Sept. 2006

[18] V. Koster, A. Lewandowski and C. Wietfeld, "Direction of Arrival Estimation for Vehicle-to-Person Communication Using Steerable Antennas," 2013 IEEE 78th Vehicular Technology Conference (VTC Fall), Las Vegas, NV, 2013, pp. 1-5

[19] T. Ohira and K. Gyoda, "Electronically steerable passive array radiator antennas for low-cost analog adaptive beamforming," Proceedings 2000 IEEE International Conference on Phased Array Systems and Technology (Cat. No.00TH8510), Dana Point, CA, 2000, pp. 101-104

[20] J. J. Luther, S. Ebadi and X. Gong, "Electrically-Steerable Parasitic Array Radiator (ESPAR) antenna design for arrays with two and three parasitically-coupled elements," 2012 IEEE Radio and Wireless Symposium, Santa Clara, CA, 2012, pp. 79-82

[21] T. Zhang, S. Y. Yao and Y. Wang, "Design of Radiation-Pattern-Reconfigurable Antenna With Four Beams," in IEEE Antennas and Wireless Propagation Letters, vol. 14, no. , pp. 183-186, 2015

[22] Z. Li, E. Ahmed, A. M. Eltawil and B. A. Cetiner, "A Beam-Steering Reconfigurable Antenna for WLAN Applications," in IEEE Transactions on Antennas and Propagation, vol. 63, no. 1, pp. 24-32, Jan. 2015

[23] W. S. Kang, J. A. Park and Y. J. Yoon, "Simple reconfigurable antenna with radiation pattern," in Electronics Letters, vol. 44, no. 3, pp. 182-183, January 31 2008

[24] W. Kang, S. Lee and K. Kim, "Design of symmetric beam pattern reconfigurable antenna," in Electronics Letters, vol. 46, no. 23, pp. 1536-1537, November 11 2010

[25] W. Kang and K. Kim, "A radiation pattern-reconfigurable antenna for wireless communications," 2011 IEEE International Symposium on Antennas and Propagation (APSURSI), Spokane, WA, 2011, pp. 1545-1548

[26] S. L. Preston, D. V. Thiel, T. A. Smith, S. G. O'Keefe and Jun Wei Lu, "Base-station tracking in mobile communications using a switched

parasitic antenna array," in IEEE Transactions on Antennas and Propagation, vol. 46, no. 6, pp. 841-844, Jun 1998

[27] S. W. Lee and Y. J. Sung, "Simple Polarization-Reconfigurable Antenna With T-Shaped Feed," in IEEE Antennas and Wireless Propagation Letters, vol. 15, no. , pp. 114-117, 2016

[28] P. Nikitin, "Wirelessly reconfigurable antenna," 2015 IEEE International Symposium on Antennas and Propagation & USNC/URSI National Radio Science Meeting, Vancouver, BC, 2015, pp. 2257-2258

[29] P. Nikitin, "Self-reconfigurable antenna", US patent application, 2015

[30] S. Lim and H. Ling, "Design of electrically small, pattern reconfigurable Yagi antenna," in Electronics Letters, vol. 43, no. 24, pp. 1326-1327, Nov. 22 2009

[31] S. Lim, "Design of a Multidirectional, High-Gain Compact Yagi Antenna," in IEEE Antennas and Wireless Propagation Letters, vol. 8, no. , pp. 418-420, 2009

[32] Z. Imran and C. Panagamuwa, "Beam-switching planar parasitic antenna array," 2014 Loughborough Antennas and Propagation Conference (LAPC), Loughborough, 2014, pp. 160-164

[33] S. K. Sharma, F. Fideles and A. Kalikonda, "Radiation pattern reconfigurable planar Yagi-Uda antenna," 2013 IEEE Antennas and Propagation Society International Symposium (APSURSI), Orlando, FL, 2013, pp. 190-191

[34] C. Kittiyanpunya and M. Krairiksh, "Pattern reconfigurable printed Yagi-Uda antenna," 2014 International Symposium on Antennas and Propagation Conference Proceedings, Kaohsiung, 2014, pp. 325-326

[35] A. Sample et. al., "Design of an RFID-Based Battery-Free Programmable Sensing Platform," IEEE Trans. on Instrumentation and Measurement, vol. 57, no. 11, pp. 2608-2615, Nov. 2008

[36] A. N. Parks and J. R. Smith, "Sifting through the airwaves: Efficient and scalable multiband RF harvesting," 2014 IEEE International Conference on RFID (IEEE RFID), Orlando, FL, 2014, pp. 74-81

[37] P. Hindle, "The State of RF/microwave Switch Devices", Microwave Journal, Nov. 2010

[38] PIN Diode Basics, application note: http://www.skyworksinc.com/uploads/documents/200823A.pdf

[39] Design with PIN diodes, application note, http://www.skyworksinc.com/uploads/documents/Design_With_PIN_Diodes_200312D.pdf

[40] M. F. Ismail, M. K. A. Rahim and H. A. Majid, "The Investigation of PIN diode switch on reconfigurable antenna," 2011 IEEE International RF & Microwave Conference, Seremban, Negeri Sembilan, 2011, pp. 234-237

[41] SMP1320 PIN diodes by SkyWorks: http://www.skyworksinc.com/Product/476/SMP1320_Series

[42] HSMS-2852 Schottky diodes by Broadcom: https://www.broadcom.com/products/wireless/diodes/schottky/hsms-2852

[43] MAX 931-934 comparator ICs by Maxim Integrated: https://www.maximintegrated.com/en/datasheet/index.mvp/id/1219

[44] P. V. Nikitin, K. V. S. Rao, R. Martinez and S. F. Lam, "Sensitivity and Impedance Measurements of UHF RFID Chips," in IEEE Transactions on Microwave Theory and Techniques, vol. 57, no. 5, pp. 1297-1302, May 2009

[45] Series-Parallel Impedance Conversion Calculator http://www.daycounter.com/Calculators/Parallel-Series-Imedance-Conversion-Calculator.phtml

[46] Ansys HFSS EM simulation software: http://www.ansys.com/Products/Simulation+Technology/Electronics/Signal+Integrity/ANSYS+HFSS

[47] Sophocles J. Orfanidis, "Electromagnetic Waves and Antennas" (book), http://www.ece.rutgers.edu/~orfanidi/ewa/

[48] T. Trick and J. Resh, "Transducer Power Gain in Optimally Matched Networks," in IEEE Transactions on Circuit Theory, vol. 14, no. 1, pp. 105-107, Mar 1967

[49] P. V. Nikitin and K. V. S. Rao, "Gain measurement of antennas using RFID," 2011 IEEE International Symposium on Antennas and Propagation (APSURSI), Spokane, WA, 2011, pp. 1012-1015

[50] Voyantic Tagformance Pro system: http://voyantic.com/products/tagformance-pro

[51] A. Michel; M. Rodriguez-Pino; P. Nepa, "Reconfigurable Modular Antenna for Near-Field UHF RFID Smart Point Readers," in IEEE Transactions on Antennas and Propagation, 2016

[52] RFID UHF SmartShelf Antenna: https://www.kathrein-rfid.de/en/new-krai-rfid-uhf-smartshelf-antenna.html

[53] C. Y. Wu, J. Du, A. K. Ren and J. Y. Li, "Large-area RFID reader antenna for smart shelf at UHF," in Electronics Letters, vol. 48, no. 15, pp. 899-900, July 19 2012

[54] A. S. Andrenko, "EM analysis of smart shelf RFID antenna with reconfigurable interrogation zone," 2016 URSI International Symposium on Electromagnetic Theory (EMTS), Espoo, 2016, pp. 569-571

[55] M. Daiki; E. Perret, "Near-Field Modular Antenna Concept with Configurable Reading Area for RFID Applications," in IEEE Transactions on Antennas and Propagation, 2016

[56] D. V. Thiel, "Impedance variations in controlled reactance parasitic antennas," 2005 IEEE Antennas and Propagation Society International Symposium, 2005, pp. 671-674 vol. 3A

[57] A. Miura, W. Luo, M. Taromaru, M. Ueba and T. Ohira, "Experimental Study of Reactively Loaded Parasitic Microstrip Array Antenna for Circular Polarization," The Second European Conference on Antennas and Propagation, EuCAP 2007, Edinburgh, 2007, pp. 1-5

[58] D. F. Kelley, "Efficient calculation of radiation patterns for reactively-steered array antennas," IEEE Antennas and Propagation Society Symposium, 2004., 2004, pp. 2635-2638

[59] "Parasitic Antenna Arrays for Wireless MIMO Systems" (book), Springer, 2014, Editors: A. Kalis, A. Kanatas, C. Papadias, http://www.springer.com/us/book/9781461479987

[60] O. N. Alrabadi, J. Perruisseau-Carrier and A. Kalis, "MIMO Transmission Using a Single RF Source: Theory and Antenna Design," in IEEE Transactions on Antennas and Propagation, vol. 60, no. 2, pp. 654-664, Feb. 2012

[61] S. V. Hum, M. Okoniewski and R. J. Davies, "Modeling and Design of Electronically Tunable Reflectarrays," in IEEE Transactions on Antennas and Propagation, vol. 55, no. 8, pp. 2200-2210, Aug. 2007

[62] J. P. Gianvittorio and Y. Rahmat-Samii, "Reconfigurable patch antennas for steerable reflectarray applications," in IEEE Transactions on Antennas and Propagation, vol. 54, no. 5, pp. 1388-1392, May 2006

[63] S. Yang, C. Zhang, H. K. Pan, A. E. Fathy and V. K. Nair, "Frequency-reconfigurable antennas for multiradio wireless platforms," in IEEE Microwave Magazine, vol. 10, no. 1, pp. 66-83, February 2009

[64] Y. E. Erdemli, R. A. Gilbert and J. L. Volakis, "A reconfigurable slot aperture design over a broad-band substrate/feed structure," in IEEE Transactions on Antennas and Propagation, vol. 52, no. 11, pp. 2860-2870, Nov. 2004

[65] A. Khaleghi and M. Kamyab, "Reconfigurable Single Port Antenna With Circular Polarization Diversity," in IEEE Transactions on Antennas and Propagation, vol. 57, no. 2, pp. 555-559, Feb. 2009

[66] L. H. Chang, W. C. Lai, J. C. Cheng and C. W. Hsue, "A Symmetrical Reconfigurable Multipolarization Circular Patch Antenna," in IEEE Antennas and Wireless Propagation Letters, vol. 13, no. , pp. 87-90, 2014

[67] S. Zhang, G. H. Huff, J. Feng and J. T. Bernhard, "A pattern reconfigurable microstrip parasitic array," in IEEE Transactions on Antennas and Propagation, vol. 52, no. 10, pp. 2773-2776, Oct. 2004

[68] X. S. Yang, B. Z. Wang, W. Wu and S. Xiao, "Yagi Patch Antenna With Dual-Band and Pattern Reconfigurable Characteristics," in IEEE Antennas and Wireless Propagation Letters, vol. 6, no. , pp. 168-171, 2007

[69] M. Jusoh, T. Sabapathy, M. F. Jamlos and M. R. Kamarudin, "Reconfigurable Four-Parasitic-Elements Patch Antenna for High-Gain Beam Switching Application," in IEEE Antennas and Wireless Propagation Letters, vol. 13, no. , pp. 79-82, 2014

[70] M. D. Gregory and D. H. Werner, "Application of the Memristor in Reconfigurable Electromagnetic Devices," in IEEE Antennas and Propagation Magazine, vol. 57, no. 1, pp. 239-248, Feb. 2015